Environmental Pollution 295 (2022) 118695

Contents lists available at ScienceDirect

Environmental Pollution

journal homepage: www.elsevier.com/locate/envpol

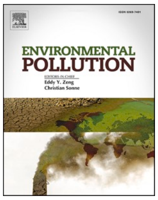

Speciation and release risk of heavy metals bonded on simulated naturally-aged microplastics prepared from artificially broken macroplastics

Gaobin Chen [a,b], Qianmin Fu [a,b], Xiaofei Tan [a,b,*], Hailan Yang [a,b], Yang Luo [a,b], Maocai Shen [a,b], Yanling Gu [c]

[a] *College of Environmental Science and Engineering, Hunan University, Changsha, 410082, PR China*
[b] *Key Laboratory of Environmental Biology and Pollution Control (Hunan University), Ministry of Education, Changsha, 410082, PR China*
[c] *College of Materials Science and Engineering, Changsha University of Science and Technology, Changsha, 410114, PR China*

ARTICLE INFO

Keywords:
Naturally-aged microplastics
Heavy metals
Speciation
Release
Risk

ABSTRACT

The negative impact of microplastics (MPs) act as metals vectors to environment and ecosystem have been paid more and more attention, and the accumulation risk of them to human body through the food chains and food webs needs to attract attention. In addition, the MPs bonded with heavy metals transport from river into the sea with high salinity may also have metals release risk. Herein, natural aged microplastics prepared from artificially broken macroplastics adsorbed with heavy metals accumulated from the natural environment were tested for their states and release risk in several simulated solution (NaCl and gastrointestinal solutions) to understand their effects on environment and human health. The adsorption capacity of different heavy metals on MPs was different during natural aging process proved by four-acid digestion method. Metals with high accumulation (including Pb, As, Cr, Mn, Ni, Zn, Co, Cu and Cd) on NAMPs were selected for further study. Results obtained via three-step extraction method showed that these heavy metals were mainly present as acid-extractable and reducible ions, which were characterized by high bioavailability. Release experiments suggested the notable Mn, Zn, As, Cr, Cu and Ni release in NaCl solution, and significant release of Mn, Zn, As, Cr, Cu, Pb and Ni in gastrointestinal solutions. The high metal release ratio in the simulated gastric solution was attributed to the weak binding of metal ions to NAMPs in acidic environment. This study will play a vital rule in assessing the ecological risks associated with MPs in natural environment.

1. Introduction

Owing to their aging and degradation under natural conditions, plastics unconsciously released into the environment transform into microplastics (<5 mm in particle size). Microplastics (MPs) negatively impact the natural environment and organisms. MPs are ingested by several aquatic fauna, thereby posing serious threats to these organisms (Ajith et al., 2020). MPs have negative effects on the health of aquatic organisms (da Costa Araujo et al., 2020) such as phytoplankton (Long et al., 2015), zooplankton (Desforges et al., 2015), and pelagic fish (Mukasa-Tebandeke et al., 2016). In addition, MPs also cause adverse reactions in fish, such as impairing their predatory ability, inhibiting lipid oxidation, reducing growth and energy reserves, and damaging the gallbladder and liver (Barboza et al., 2018; Ferreira et al., 2016; Yin et al., 2018). MPs are harmful to phytoplankton, zooplankton and even fish, so there are also potential risks to accumulate to higher levels and even among consumers through the food chain food network.

Studies have shown that MPs have the ability to adsorb and accumulate various pollutants from the environment (Shen et al., 2019), especially the aged MPs. Compared with large plastics, MPs are characterized by large surface areas, elevated porosity, and higher hydrophobicity (Dong et al., 2019; Liu et al., 2020), which enhance their contaminant adsorption abilities. Compared with commercialized MPs, the higher negatively charged surfaces of naturally-aged MPs (NAMPs) and higher hydrophilicity enhance their ability to adsorb pollutants such as heavy metals in aquatic environments (Salehi et al., 2018). According to the experimental studies, MPs serve as heavy metal carriers, with higher adsorption as the polarity and surface area increase (Brennecke

---

* Corresponding author. College of Environmental Science and Engineering, Hunan University, Changsha, 410082, PR China.
E-mail address: tanxf@hnu.edu.cn (X. Tan).

https://doi.org/10.1016/j.envpol.2021.118695
Received 26 July 2021; Received in revised form 21 November 2021; Accepted 14 December 2021

et al., 2016; Zhou et al., 2019). Besson et al. (2020) reported that the adsorption capacities of Cd, Cs, and Zn on pristine polyethylene (PE) MPs are higher than those of sediment particles. According to previous studies, aging promotes the combination of non-polar and polar pollutants, thereby promoting the migration of contaminants (Liu et al., 2019). In fact, NAMPs adsorb higher amounts of metals (e.g., silver) than pristine MPs, and subsequently yield more metals during leaching (Kalcikova et al., 2020). Previously, higher adsorption capacities of trace metals on aging PE than that on pristine PE has been reported (Kalcikova et al., 2020). However, further experiments are required to elucidate the differences in the adsorption capacities of aging and pristine MPs.

As metal ion vectors, MPs promoted the accumulation of toxic substances in aquatic environments. Meanwhile, the heavy metals adsorbed to the NAMPs were at risk of release. Owing to the wide occurrence of heavy metals in aquatic environments, their potential to negatively affect human health through direct accumulation, i.e., from drinking water, or indirect accumulation, i.e., through crops, marine organism, etc, cannot be neglected (Sharma et al., 2019). Heavy metals can be hyperaccumulated in the root of oilseed crops, negatively affect the survival and fecundity of zooplankton, and damage the health of higher organisms in a food chain (Almeida et al., 2020; Bassegio et al., 2020; Vroom et al., 2017). The presence of Pb(II) can result in kidney damage or cancer (Tang et al., 2020), while that of As results in chronic health problems, including neurological diseases (Bessaies et al., 2020; Cui et al., 2016). As co-pollutants, MPs and heavy metal eventually reach organisms via ingestion (Browne et al., 2013; Wright et al., 2013) and cause harm to humans (Zhou et al., 2020), such as impairing the nervous system (Biamis et al., 2021), promoting cytotoxicity, and causing morphological changes (Wu et al., 2019). Therefore, determining the characteristics, sources, and health hazards of pollution is crucial to reduce risk to human.

Considering that desorption is an interfacial process, it is available for investigating the stability and ecological risk of pollutants adsorbed by MPs in aquatic environments. The presence of PE MPs in the gut of an organism is reported to increase the desorption rate of metal ions such as Zn (Hodson et al., 2017). In addition, Cd(II) adsorbed on PE MPs can be easily desorbed in aqueous solution with different contact time, solution pH, particle size, and salinity (Wang et al., 2019). Although there are several studies on the adsorption–desorption characteristics of MPs and heavy metal ions, the stability and potential release potential of heavy metal ions adsorbed on NAMPs has not been investigated in detail.

Therefore, in this study, we used the artificially broken naturally-aged macroplastics to simulate the naturally-aged MPs (NAMPs). The stability of the adsorption between NAMPs and heavy metals, as well as their impacts in the background of the human digestive solutions, are investigated. This study aims to: (1) detect the types of heavy metals adsorbed on NAMP accumulated from the environment; (2) determine different states of heavy metals adsorbed on NAMPs; (3) analyze the release of heavy metals with high accumulation (As, Pb, Cr, Ni, Co, Zn, Mn, Cu and Cd) in solution with different salinity and simulated gastrointestinal solutions of the human digestive system, and (4) highlight the properties of NAMPs as heavy metal carriers and potential pollution sources.

2. Methods and materials

2.1. Materials

The natural-aged (beached) plastics were collected using pickup device from the bottomland of central section of the Xiangjiang River in Hunan Province, China. During the collection process of natural-aged plastics, we mainly choose plastics of transparent film material with attached biofilm and without color. Large pieces of plastic which had organic matter and attached particles as more as possible on the surface was chosen for the experiment. Reference to the previous study, the plastics were soaked in ultra-pure water to carefully remove the surface sand (Ye et al., 2020). After drying, the sample was cut below 5 mm in diameter with scissors, then screened through 10 mesh to obtain simulated NAMPs used in the study. The picture of the obtained NAMPs is shown in Fig. S1. Before experiment, we prepared enough NAMPs for the whole study using the same kind of plastics and the obtained NAMPs were evenly mixed to reduce the experimental error caused by different plastics.

Sodium chloride (NaCl), sodium hydroxide (NaOH), sodium carbonate (Na_2CO_3), calcium chloride ($CaCl_2$), acetic acid (CH_3COOH), hydroxylamine hydrochloride ($HONH_2HCl$), nitric acid (HNO_3), hydrogen peroxide (H_2O_2), ammonium acetate (NH_4CH_2COOH), hydrofluoric acid (HF), and perchloric acid ($HClO_4$) were purchased from Sinopharm Chemical Reagent Co. Ltd., China. HNO_3, HF, and $HClO_4$ were of guaranteed reagent (GR) purity, while all the other reagents were of analytical reagent (AR) grade. The concentrations of ions in different solutions were measured by inductively coupled plasma mass spectrometry (ICP-MS; Agilent 7900, Japan).

2.2. Characterization of MPs

To characterize and evaluate the release mechanisms of MPs, several methods were employed. Suitable amount of evenly mixed NAMPs was used for the following analysis. Scanning electron microscopy (SEM; TESCAN MIRA4, Tesken, Czech) and optical microscopy (OM; OLYMPUS CX31 RTSF, Japan) were utilized for examining the morphology of MPs surfaces. Elemental mapping of microstructures of MPs was analyzed by SEM-energy dispersive X-ray spectrometry (SEM-EDS; Xplore, Oxford, UK) before and after being soaked in nitric acid solution (pH = 2) for 7 days. Fourier transform infrared spectroscopy (FTIR; NICOLET5700 FT-IR spectrometer, United States) was used for the identification of polymer type. X-ray diffractometry (XRD; Brucker D8 Advanced, Germany) was used to identify the quartz and other phases on MPs surface. X-ray photoelectron spectrometry (XPS; ESCALAB250XI, SEMEL technology, United States; binding energy in C1s 284.8 eV calibration) were used for characterizing the MPs before and after immersion in simulated gastrointestinal solutions.

2.3. Determination of different heavy metals on MPs

In order to determine the heavy metals on MPs surface, 0.01 mol/L HNO_3 solution (pH = 2) was used for heavy metals release while not able to dissolve the PMs particles. The MPs (75 mg) were added into conical flask containing 150 mL HNO_3 solutions. Then the experiments were conducted in a vertical constant temperature air shaker at ambient temperature (298 K) and pressure, at a shaking speed of 160 rpm. The samples were taken out at different time intervals, and passed through 0.45 μm membrane filters, then diluted using HNO_3 before testing. After reaction for 7 d, the MPs were separated from solution and dried in oven at 60 °C for 24 h. The obtained MPs were tested using optical microscopy, SEM-EDS, FTIR and XRD. The residual contents of heavy metals in MPs after being soaked in nitric acid solution (pH = 2) for 7 days was determined by four-acid digestion method.

2.4. Sequential extraction of heavy metals on MPs

Three-step sequential extraction from the Community Bureau of Reference (BCR) was used to measure different forms of metal ions of soil and sediment (Zemberyova et al., 2006). And the modified processes used in this study can be summarized as follows:

Step one (acid-extractable metal ion content determination): Approximately 40 mL CH_3COOH (0.11 M) was added to 1 g of a dried MPs sample in a centrifuging tube. The tube was then placed in a shaker for 22 h (150 rpm) at 298 K. After reaction, the tube was placed in a centrifuge and centrifuged at 6000 rpm for 10 min. The supernatant was sucked out using a syringe and the obtained solution was diluted using

Milli-Q water and stored at 277 K for subsequent analysis. The solid residues were washed twice using Milli-Q water and utilized in next step.

Step two (reducible metal ion content determination): Approximately 30 mL $HONH_2HCl$ (0.5 M) and HNO_3 (0.05 M) mixture was added to the tube containing the residual solids and shaken for 22 h (150 rpm) at 298 K. After reaction, the tube was placed in a centrifuge and centrifuged at 6000 rpm for 10 min. The supernatant was sucked out using a syringe and the obtained solution was stored at 277 K until analysis, while the residual solids were cleaned and used in step three.

Step three (oxidized metal ion content measurement): Approximately 10 mL H_2O_2 with its pH adjusted 2.0 using HNO_3 (0.1 M) was added to the residual solid. The mixture was stirred at 298 K for 1 h, and then held at 358 K for 1 h. The lid of tube was opened, and the mixture was heated until the volume decreased to about 5 mL. And then, 10 mL H_2O_2 was added to the tube and kept at 358 K for 1 h. The lid of tube was then reopened and the mixture was heated until the volume was less than 3 mL. After cooling to room temperature, approximately 30 mL CH_3COONH_4 (1.0 M, pH = 2.0) was added to the solution, and the tube was shaken (150 rpm) for 22 h at 298 K. The extraction in step one was repeated to obtain a solution for testing the organically bound components.

Four-acid digestion method (using HCl, HNO_3, HF, and $HClO_4$) was used to measure the total content of different heavy metals of MPs including the heavy metals on their surface and in their structures themselves. The detailed steps of digestion are as follows: 0.5 g NAMPs samples were placed in digestion tank and mixed with 0.5 mL Milli-Q water and 5 mL HCl. After thoroughly homogenized by shaking, mixture was held at 393 K for 2 h in an automatic graphite digestion instrument (Gedana DS-72, China). After cooling, 8 mL of HNO_3, 5 mL of HF, and 3 mL $HClO_4$ were added into digestion tank and mixed well with shaking. The mixture was heated at 403 K for 80 min, and then the temperature was increased to 423 K and maintained for 60 min. After further shaking, the tank was heated to 438 K and held isothermally to dissolve all solids. The remaining solution was diluted with deionized water and filtered through a 0.45 μm filter membrane for subsequent testing. The experiment process was repeated three times to reduce the errors.

The metal concentrations measured after the four-acid digestion minus the acid-extractable, reducible, and oxidized ions concentrations for each metal provided the residual concentration. The modified three-step sequential extraction three-step sequential extraction from Community Bureau of Reference (BCR) enabled the analysis of metal contents associated with the following forms (Zemberyova et al., 2006): 1) Acid-extractable ions involving the coprecipitation binding of heavy metals in soils on carbonate minerals; and 2) Reducible metal ions linked to mineral exosomes and fine dispersed particles. Owing to the high specific surface areas of active ferromanganese oxides, these easily adsorbed or co-precipitated anions. 3) Oxidized ions linked to chelation with organic matter and sulfides; and 4) Residual ions in crystal lattices of soils that were hardly absorbed by plants.

2.5. *Release risk of heavy metals on MPs*

To assess the effect of ionic strength on the surface stability of heavy metals on MPs, NaCl with different concentrations (0, 50, 100, and 200 mg L^{-1}) were used. After sampling, the obtained solution was passed through 0.45 μm membrane filters and diluted 10 times before detection using ICP-MS. Then, a background solution (0.01 M $CaCl_2$, pH = 6.6), simulated intestinal solution (SIS, 0.12 M NaCl and 0.02 M Na_2CO_3, pH = 7.5), and simulated gastric solution (SGS, 0.1 M NaCl prepared using the background solution above, pH = 2.0) were utilized to investigate the stability of metal ions on the surfaces of NAMPs in simulated environments at 310 K. The solutions for release were adjusted to the desired pH values using NaOH (0.01 M and 0.1 M) or HNO_3 (0.01 M and 0.1 M). Batch release experiments were conducted in a vertical constant temperature air shaker at ambient temperature (298 K) and pressure, at a shaking speed of 160 rpm. Samples were then taken from the 150 mL solutions containing 0.5 g L^{-1} of MPs at different time intervals. After passing through 0.45 μm membrane filters, the samples were diluted using HNO_3 before testing. Each experiment was repeated three times. After reaction for 7 d, the MPs were separated from solution and dried in oven at 60 °C for 24 h. The obtained MPs were tested using optical microscopy, SEM-EDS, FTIR and XRD.

2.6. *Statistical analysis*

The calculated means amount of the released metals in NaCl solution of different concentrations, released amount of metals in SIS and SGS solutions at different times, and the results of sequential extraction of heavy metals on MPs were analyzed for statistical significance by One-Way ANOVA followed by LSD and Duncan's test for multiple comparison. Differences in the released amount of metals were considered statistically significant when $p < 0.05$. Statistical analysis was performed using SPSS Statistics 27.

3. Results and discussion

3.1. *Characteristics of microplastics*

3.1.1. *Characterization of NAMPs*

The surface morphologies of the NAMPs were analyzed by SEM and OM (shown in Fig. 1 and Fig. 2). The images obtained at different magnification clearly exhibit organic layers with fluffy structures on the front and side surface of NAMPs. These layers enhanced the specific surface area values of MPs (Rozman et al., 2021) and provided sites for heavy metal adsorption for NAMPs (Ye et al., 2020), thereby improving the chances of interaction between the NAMPs and heavy metals in the environment.

FTIR spectrum of a representative NAMPs sample, as shown in Fig. 3a, exhibits six prominent peaks including 717, 2915, 1471, and 2846 cm^{-1} which are the characteristic peaks of polyethylene (PE). 1643.1 cm^{-1} and 1007.61 cm^{-1} were assigned to the stretching vibration of carbon–oxygen double bond (C=O) and silica. These results indicated that the main source of NAMPs collected is PE, which was also confirmed using XRD (Fig. 3b). The XRD data for the unused NAMPs were processed using the MDI Jade software, and the results were compared with the standard results. The peaks displayed by the NAMPs sample corresponds to $(CH_2)_x$ (PDF#40–1995) and Quartz SiO_2 (PDF#46–1045), with the $(CH_2)_x$ peak area indicating PE dominance. The presence of SiO_2 suggested a non-conforming soil particle attached to the plastics.

3.1.2. *Content and speciation of heavy metals on naturally-aged microplastics*

After being soaked in nitric acid solution (pH = 2) for 7 days, most particles were dissolved in the solution and the surface of MPs became much cleaner (Fig. 2). Most metals on MPs were released into the solution after being soaked in nitric acid solution, and the released amount increased with soaking time (Fig. S2). The tested As, Cr, Cu, Ni, Zn, and Cd reached their release equilibrium in 7 d, while Pb, Mn and Co did not. The order of release quantity is Mn > Zn > Ni > Cu > Pb > As > Cd > Co > Cr. The residual contents of heavy metals in MPs after being soaked in nitric acid solution (pH = 2) for 7 days was determined by four-acid digestion method. It was found that some heavy metals were still detected in MPs (Fig. S3). This might be due to that some minerals, such as talcum, and some plasticizer are often used during plastic product to enhance its performance, which contain some heavy metals. In addition, some heavy metals were still remained on MPs surface as they were not completely removed from MPs.

The total content of metals of the NAMPs were measured after four-acid digestion method. The accumulation capacity of MPs to different metals was different. Totally fifteen metals were detected and the

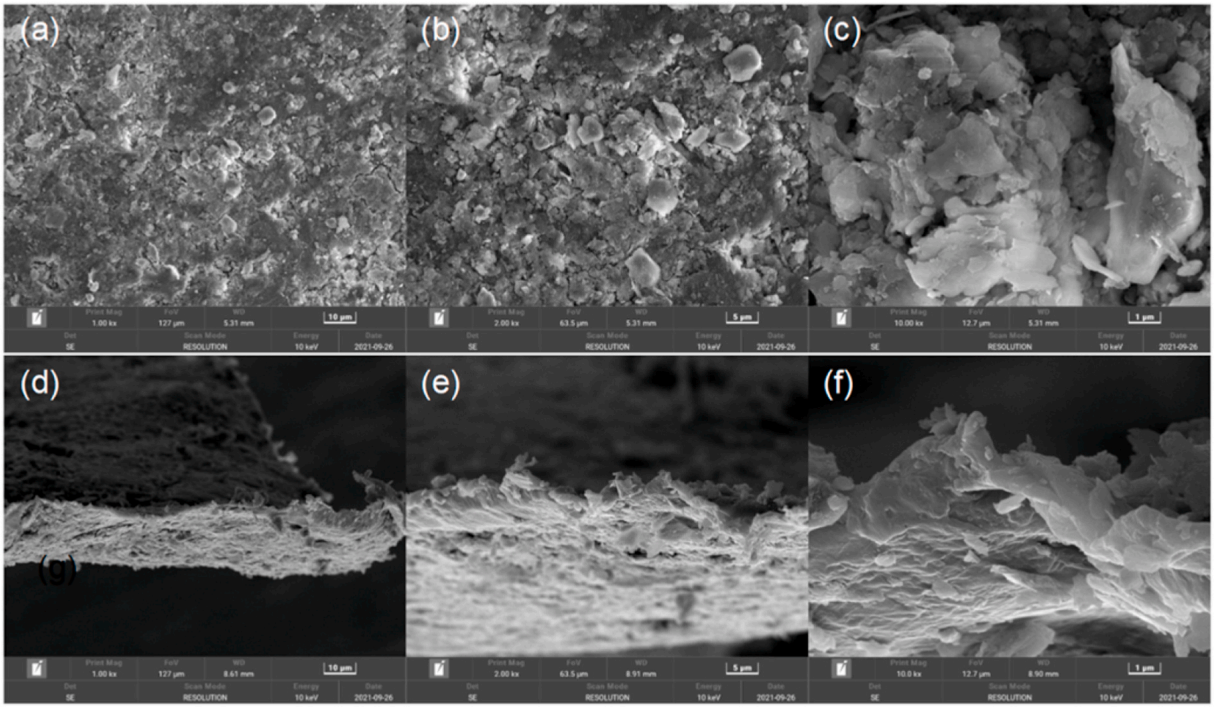

Fig. 1. SEM images of (a–c) front and (d–f) side of naturally-aged microplastics (NAMPs).

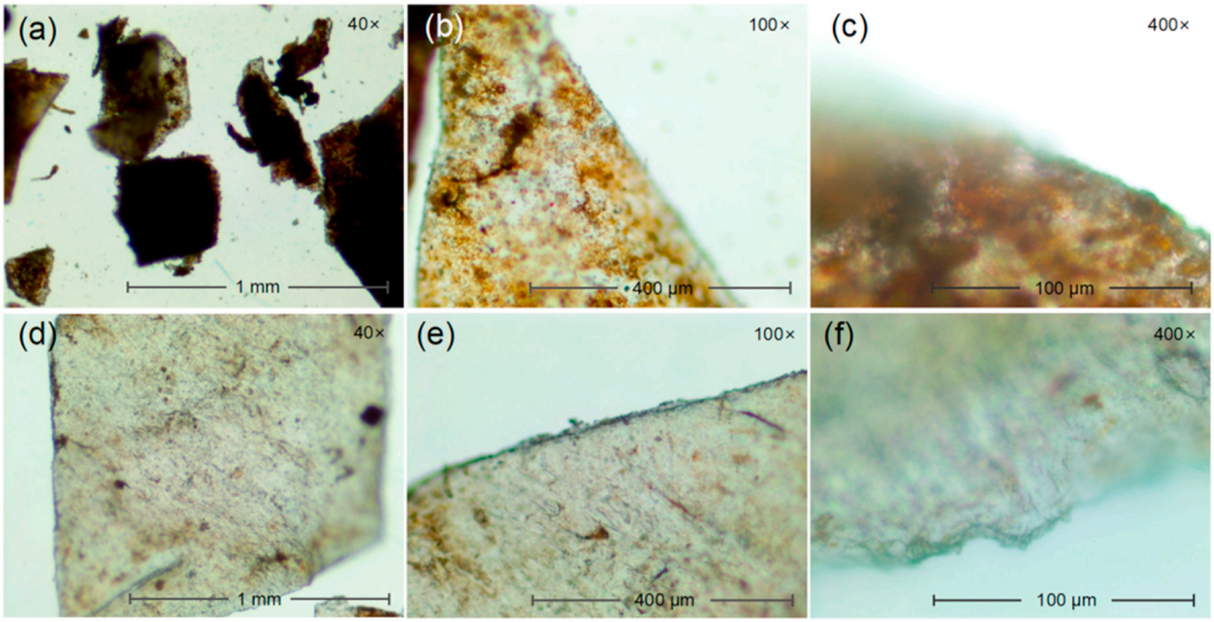

Fig. 2. Optical microscopy images of NAMPs (a–c) before and (d–f) after being soaked in nitric acid solution (pH = 2) for 7 days.

concentrations of Cr, Pb, As, Ni, Co, Zn, Mn, Cu and Cd were the nine highest concentrations among all the heavy metals. The results from measurements after the sequential extraction for the nine heavy metals are shown in Fig. 4 and Fig. 5. The total content of heavy metals on the MPs and compared with other studies are shown in Table S2. As can be seen, the content of Mn and As in our tested MPs are much higher than that of other studies (El Hadri et al., 2020; Gao et al., 2019), while the content of Cr and Pb are significantly lower than that of other studies (El Hadri et al., 2020; Guo and Wang, 2021).

According to the data shown in Fig. 4 and Table S1, before the release experiments, the residual concentrations of the nine heavy metals (Cr = 1.185, Cu = 0.45, As = 0.887, Ni = 0.618, Co = 0.159, Zn = 3.851, Mn = 281.85, Pb = 0.49 μg g^{-1}, and Cd = 0.113 μg g^{-1}) were less than 10% of the total concentrations. Among the nine heavy metals, the highest fractions were obtained from the reducible metal ions samples for Cr, Cu, Mn, Pb, Co and As, with values of 54%, 57%, 62%, 68%, 78% and 79%, respectively. However, the acid-extractable metal was the dominant speciation for Ni, Zn and Cd. Acid-extractable and reducible metal ions are more bioavailable forms of the tested metals, which accounted for more than 84% of the total amounts, except for Cr (61% of the total amounts). In addition, the high concentration of acid-extractable Mn and Zn was also noteworthy. This form of toxic metals was sensitive to

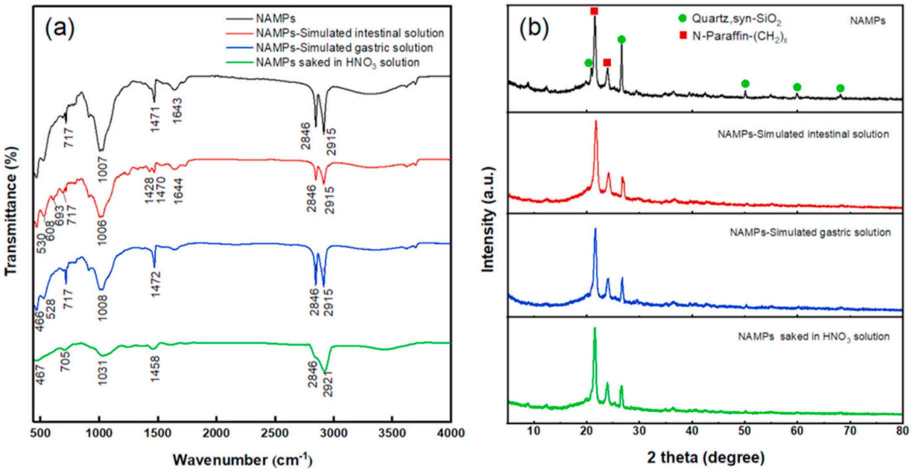

Fig. 3. (a) FTIR spectra of NAMPs, NAMPs-SIS, NAMPs-SGS and NAMPs-HNO$_3$; (b) XRD traces of the NAMPs, NAMPs-SIS, NAMPs-SGS and NAMPs-HNO$_3$.

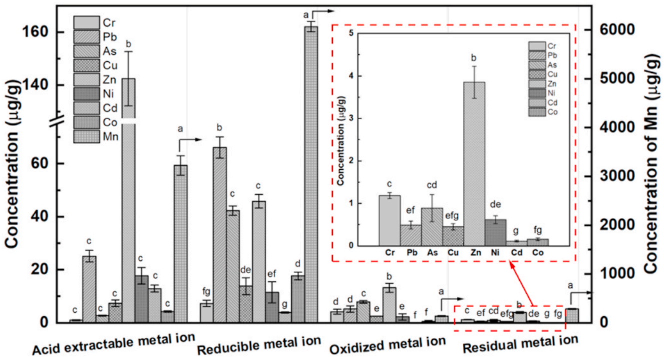

Fig. 4. Heavy metal concentrations in each fraction of the Community Bureau of Reference extracts. The insert chart shows the residual form of different metals.

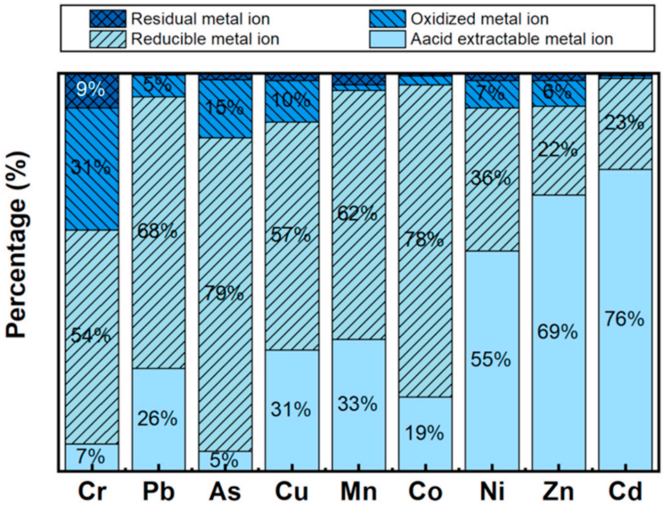

Fig. 5. The distribution of heavy metal based on various extracts.

environmental changes, and it was easily transported, transformed, and absorbed by plants (Gupta, 2016). Therefore, the sequential extraction experiments demonstrated that if MPs were transported into an aquatic environment, some heavy metals can release into the water and eventually enter the body, thereby negatively affecting human health.

3.2. Release risk of heavy metals on naturally-aged microplastics

3.2.1. Effect of ionic strength

In the body fluid environment, the presence of salts may affect the heavy metals desorption capacities of NAMPs. Herein, the release of nine metals (As, Pb, Cr, Ni, Co, Zn, Mn, Cu and Cd) from the NAMPs varied at different NaCl concentrations (shown in Fig. 6). Depending on the ionic strength of a solution, the salting-out effect was beneficial for metal adsorption, whereas the squeezing effect was unfavorable (Yin et al., 2019). Thus, release was a dynamic process involving the simultaneous release and adsorption of heavy metals. What we did not expect was that little amount of Cd (not detected in solution) was released into the NaCl solution, while different amount of As, Pb, Cr, Ni, Co, Zn, Mn and Cu was released. As shown in Fig. 6, the continuous release of As, Cr, Cu, Mn and Zn on the NAMPs into the solution occurred with time while Co, Pb and Ni displayed inconspicuous changes.

3.2.2. Effect of gastrointestinal solution

NAMPs potentially enter the human body through the food chain. Therefore, release of the studied metal ions from NAMPs was investigated in a simulated human gastrointestinal environment by configuring simulated solution. In Fig. 7, the effects of SIS and SGS on the ions release were different. However, in both simulated solutions, these metals exhibited obvious release compared to their initial concentrations over time, and displayed different changes among nine metals. These behaviors were consistent with results obtained from BCR extraction. Acid-extractable and reducible metals ions represented the dominant proportions, which highlighted the high bioavailability of these metals, thereby supporting their relatively elevated release in SGS. The release of metals displayed an increasing trend for SGS solution, and the effect of SGS on metals appeared more significant than that of SIS. The As release in SIS was more obvious over time than other metals. The presence of CO_3^{2-} in the SIS can promote the desorption of As, since CO_3^{2-} can compete for binding sites in NAMPs (Guo et al., 2013), thereby enhancing the release of As from the NAMPs. The release concentration of Mn from SIS reached its maximum within 48 h, followed by the adsorption of Mn by NAMPs with an increase in time, and eventually attaining an adsorption–desorption equilibrium. Conversely, in SGS, the release of Mn continuously increased with time. The release concentration of Pb and Ni from SIS did not change significantly during the reaction time. But in SGS, the release concentration of Pb and Ni increased over time. The increasing release concentration may be attributed to the negative surface charges of the NAMPs (Fu et al., 2021) and different metal properties. Moreover, the redox potential increased with decreasing pH, which was unfavorable for the interaction of the metal cations and NAMPs. It is expected that high proportions of

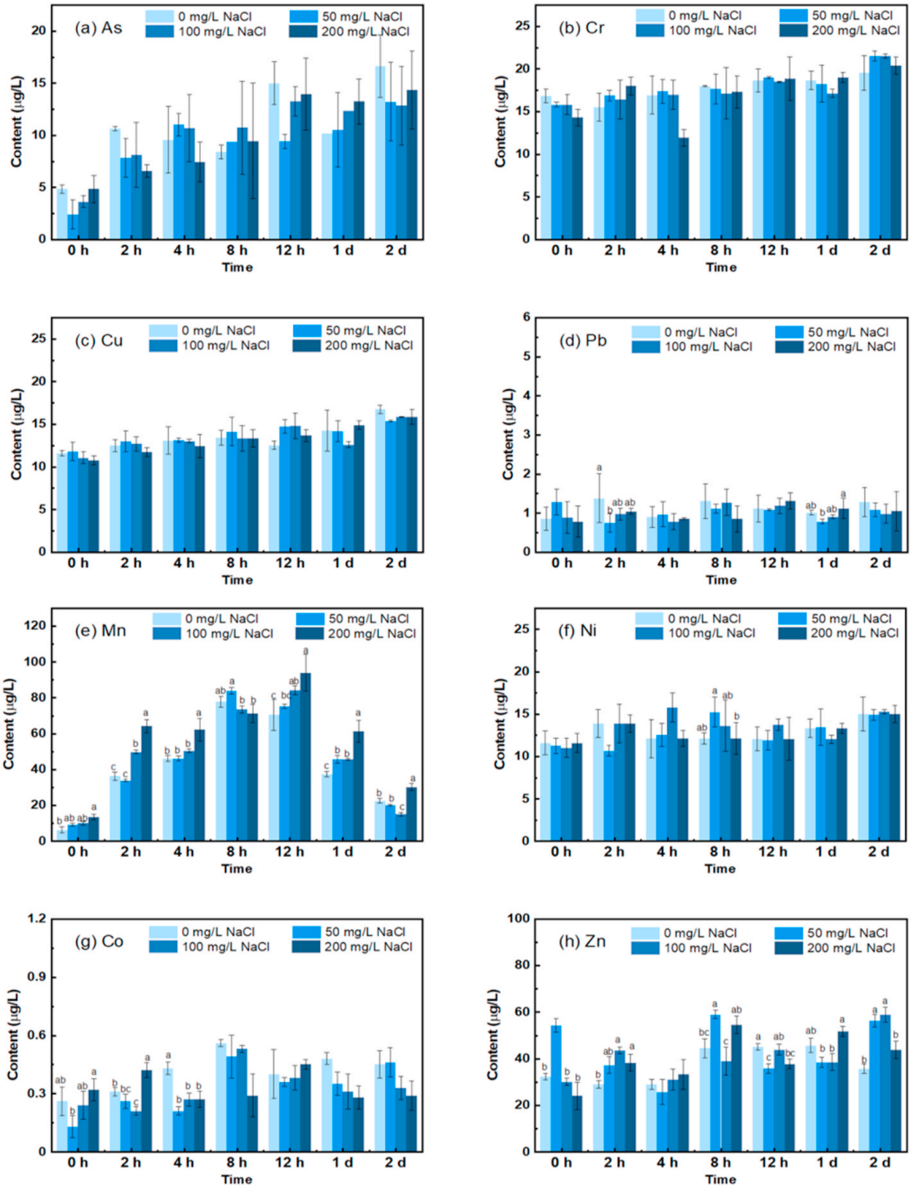

Fig. 6. Plots showing the effects of ionic strength on the release of heavy metals from naturally-aged microplastics including (a) As, (b) Cr, (c) Cu, (d) Pb, (e) Mn, (f) Ni, (g) Co and (h) Zn.

acid-extractable form of heavy metals should release more in SGS solution. However, the results in this study did not support this assumption. This might be due to that the simulated gastric solution (SGS) contained 0.1 M NaCl and 0.01 M $CaCl_2$ ($pH = 2.0$), which made the release process more complex. And each polymer has a different capacity of adsorption for heavy metals. In addition, the release potential of cationic and anionic metals in these systems might be different.

3.2.3. Release ratio

Due to the different initial content of the metals of the NAMPs, the release ratio of nine metals from NAMPs in different stimulated solutions was calculated to compare the release potential of the different metals in different solution environments. The release ratio (r, %) was equal to the release content (R, μg) of the metals in different solution environments versus the initial content (I, μg) on the NAMPs. In the formula, c ($\mu g\ L^{-1}$) is the release-concentration of the metals in solutions and i ($\mu g\ g^{-1}$) is the initial content on each gram of NAMPs (equation (1)).

$$r = \frac{R}{I} = \frac{300c}{g \cdot i} \tag{1}$$

The calculated results are shown in Table S3. The release ratio of nine metals from NAMPs reached a maximum in the simulated gastric solution (97.80% Cr, 14.68% Pb, 40.77% As, 55.08% Cu, 35.64% Mn, 42.83% Ni, 52.93% Zn, 15.22% Co, and 20.00% Cd). In simulated intestinal solution, release ratio of Cr was significantly higher than other metals and reached 74.00%. Besides, Cr was more easily desorbed in other simulated solution than other metals. Especially, the release ratio of Cr, which in the range of 43.08%–51.60%, in different concentrations of NaCl solutions were much higher than other metals, and followed by Cu whose release ratio was in the range of 19.10%–20.79%. Release ratio of Cr and Zn increased with NaCl solution concentrations, while Co showed the opposite trend. And there is no obviously difference of Pb, As, Cu, Mn and Ni in different NaCl solution. It may be related to the charge of the ions, electronegativity and other metal properties.

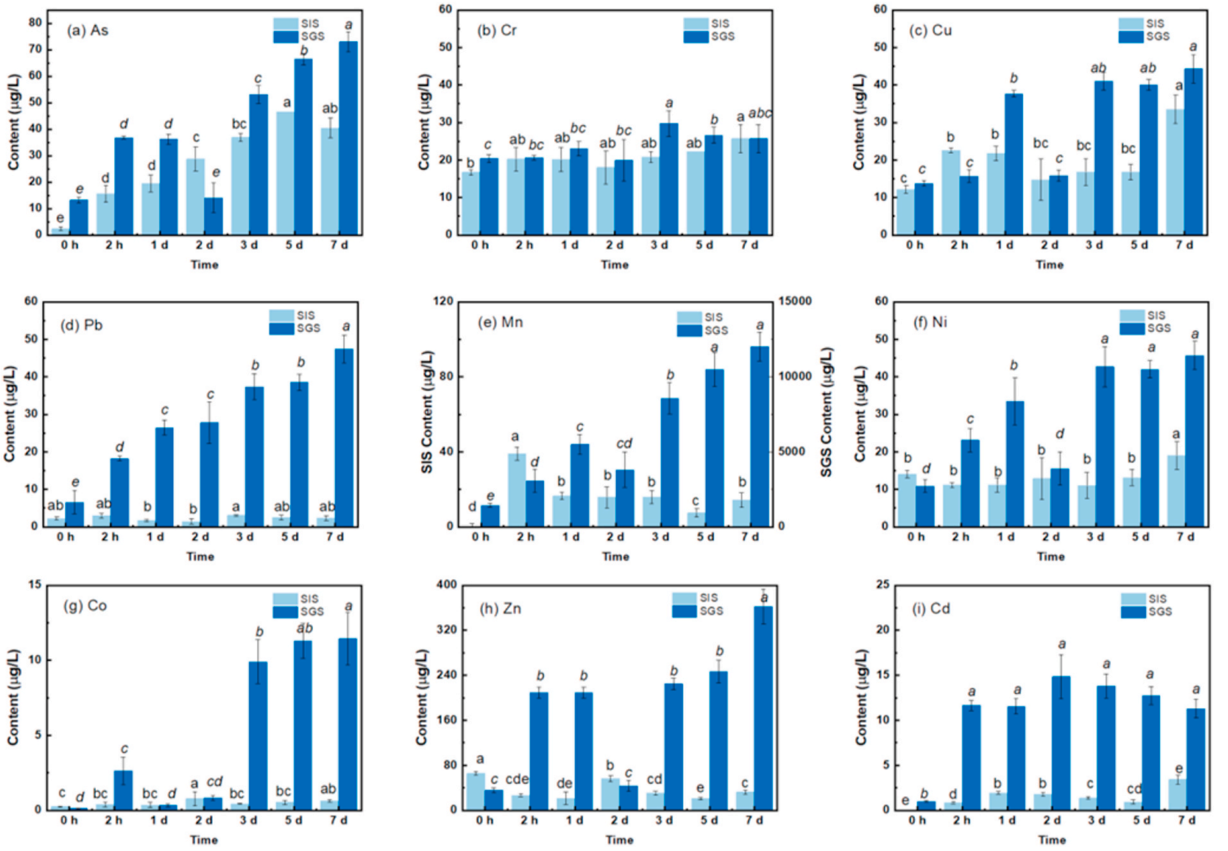

Fig. 7. Plots demonstrating the effects of gastrointestinal solutions on the release of heavy metals from naturally-aged microplastics including (a) As, (b) Cr, (c) Cu, (d) Pb, (e) Mn, (f) Ni, (g) Co, (h) Zn and (i) Cd.

3.3. Release mechanism

XPS spectra of the NAMPs surfaces, shown in Fig. 8, display C1s peaks at 284.5 eV (CH$_2$–CH$_2$), 284.9 eV (C–C), 285.4 eV (C═C), and 287.8 eV (C═O), and O1s peaks at 532.8 eV (Si–O–Si), 532.3 eV (C–OH and CO–), 531.6 eV (C–O) (Hao et al., 2021; Li and Yao, 2020; Ma et al., 2021; Ma et al., 2019; Misran et al., 2018; Qiao et al., 2018; Sun and Wen, 2020; Zhao et al., 2021). The C1s and O1s peaks of the XPS spectra of NAMPs after exposed to the simulated gastrointestinal solutions was shifted slightly. The C1s peaks for NAMPs exposed to the SIS (NAMPs-SIS) exhibited a shift of 0.5 eV to the right for C═C at 285.4 eV, while the peak initially at 287.8 eV shifted to 288.04 eV. The peak at

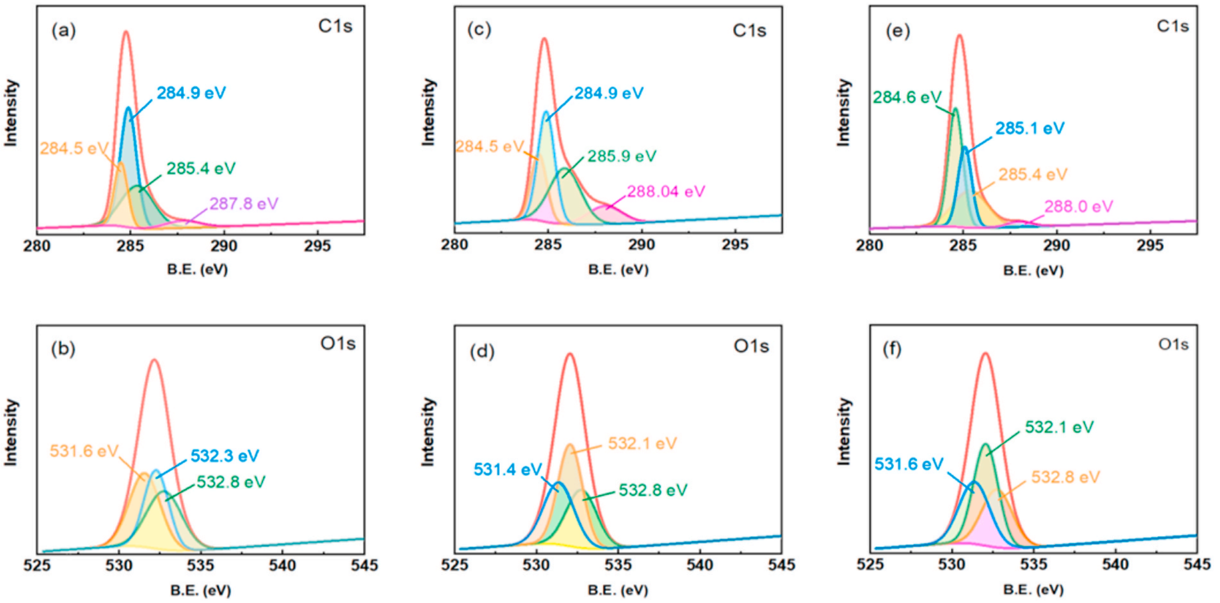

Fig. 8. XPS spectra for (a) C1s of the naturally-aged microplastics (NAMPs), (b) O1s of the NAMPs, (c) C1s of the NAMPs-simulated intestinal solution (SIS), (d) O1s of the NAMPs-SIS, (e) C1s of the NAMPs-simulated gastric solution (SGS), and (f) O1s of the NAMPs-SGS.

285.9 eV was assigned to C–OH, while that at 288.04 eV was still assigned to C═O (Sahu et al., 2012; Sethumadhavan et al., 2020). The O1s peaks revealed no change in the binding energy at 532.8 eV, indicating that the sand and gravel particles associated with the NAMPs participate minimally in the interactions between the heavy metals and NAMPs (Misran et al., 2018). This phenomenon was also reflected in the binding energy data for the NAMPs that were exposed to the SGS (NAMPs-SGS). However, the C–O signal at 531.6 eV shifted slightly by 0.2 eV–531.4 eV, and this was assigned to C═O. In the binding energy data for the SIS-exposed samples, the peaks at 285.9 eV (C–OH) and 531.4 eV (C═O) were assigned to CO_3^{2-}. This phenomenon confirmed the earlier observation that CO_3^{2-} in the SIS competed with As for active sites of NAMPs, thereby occupying the original positions of some heavy metals. After immersing the NAMPs in the SGS, the C–C signal at 284.9 eV shifted to the right by 0.2 eV to produce a C═C signal. The C═O signal at 287.8 eV also shifted to the right by 0.2 eV, but remained a C═O signal, similar to the response after treatment in the SIS. Then O1s peaks at a binding energy of 532.3 eV shifted to the left by 0.2 eV, similar to that for the treatment in the SIS, while the new peak at 532.1 eV was assigned to the presence of water in crystals.

Regarding the FTIR data, compared with the NAMPs, the NAMPs-SIS and NAMPs-SGS data showed new peaks between 450 and 650 cm^{-1}, which were similar to those at 466, 528, 530, and 608 cm^{-1}, and these small peaks were assigned to SiO_2 (Hayati-Ashtiani, 2011; Jiang et al., 2019; Mukasa-Tebandeke et al., 2016; Nikitin and Khriachtchev, 2015; Young et al., 2000; Zhang et al., 2019). In the FTIR spectrum of the NAMPs-SIS sample (Fig. 3a), two new peaks were present at 693 and 1428 cm^{-1}. These peaks were considered as CO_3^{2-} vibration peaks, which is consistent with the XPS results and further confirms the competition for active sites by the CO_3^{2-} in SIS. In the spectrum of the NAMPs-SGS sample, the original peak at 1643 cm^{-1} attributed to the presence of water in crystals disappeared. This shift in position may be caused by the acidic SGS changing the original binding form of the water in crystals. The peaks between 450 and 650 cm^{-1} which were assigned to SiO_2 were became much smaller after nitric acid solution treatment, suggesting that most inorganic particles were removed from the surface of MPs. Moreover, The XRD traces revealed that compared with the NAMPs sample, the main peaks in the NAMPs-SIS, NAMPs-SGS and NAMPs-HNO_3 samples were similar (Fig. 3b). This proves that the original crystal structure of the NAMPs was preserved after the release experiments, indicating that the organic matter attached to the surfaces of the MPs during aging may be active in the process. The intensity of quartz solid peak at about $2\theta = 26^\circ$ significantly decreased after SIS, SGS and HNO_3 treatment, which also confirmed the removal of minerals particles from MPs.

In order to distinguish the fine particle and organic matter on MPs, elemental mapping of microstructures of MPs was analyzed by scanning electron microscopy-energy dispersive X-ray spectrometry (SEM-EDS) before and after being soaked in nitric acid solution (pH = 2) for 7 days. Si was regarded as the representative element of sediment particles on the surface of MPs, and C was regarded as the representative element of organic matter on the surface of MPs or matrix of MPs. As can be seen from Fig. 9 and Fig. S4, a lot of Si element (7.25 wt%) was existed on the NAMPs surface, which suggested that many mud or sand particles (SiO_2 as main component) were attached on the MPs surface (can be also seen from Fig. 2). About 90.28 wt% of C on MPs surface suggested the existing of some organic matter on the surface and the exposure of MPs matrix. Mn, As and Pb could be obviously observed in the mapping image. Comparing the elemental mapping of Si, C, Mn, As and Pb, we could infer that these metals were mainly combined with the inorganic mineral particles, and some of which were bonded with organic matter on the MPs. After being soaked in nitric acid solution (pH = 2) for 7 days, most particles were dissolved in the solution and the surface of MPs became much cleaner (Fig. 2). Most metals on MPs were released into the solution after being soaked in nitric acid solution, and the released amount increased with soaking time (Fig. S2). The content of C on MPs surface increased to 97.76 wt%, while Si element decreased to 1.26 wt% (Fig. S4). However, some stable particles were still firmly attached onto the MPs surface (Fig. S5). A small amount of residual Mn, As and Pb were observed. By comparing the elemental mapping of Si and Mn, we could also see that the residual Mn was mainly combined with the inorganic mineral particles on the MPs. The dissolution of the mineral particles bonded with metals might be an important reason for the release of metals.

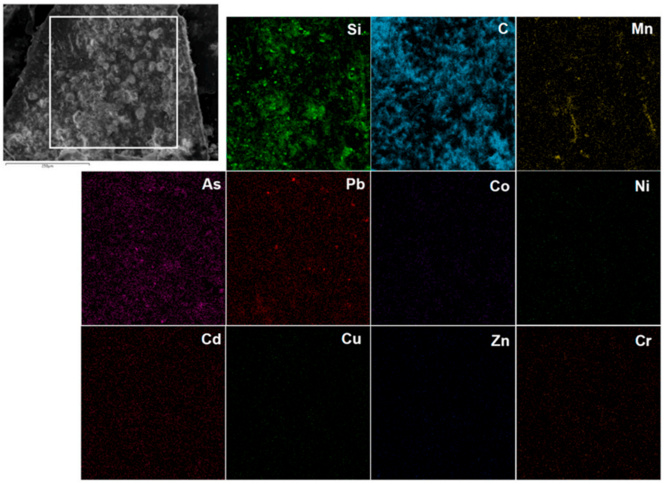

Fig. 9. Elemental mapping of microstructures of NAMPs analyzed by scanning electron microscopy-energy dispersive X-ray spectrometry (SEM-EDS).

4. Conclusion

Herein, heavy metals adsorbed by NAMPs under natural conditions, after transportation to aquatic environments in different salinity and simulated gastrointestinal solutions of the human digestive system, was investigated and their possible release mechanisms were proposed. NAMPs can accumulate different heavy metals including As, Pb, Cr, Mn, Ni, Zn, Co, Cu and Cd from the environment. High proportion reducible and acid-extractable metal form suggested that they could be easily desorbed into stimulated solutions from the NAMPs. CO_3^{2-} in SIS was active during the desorption of heavy metals by competing for binding sites between the metal ions and NAMPs. In SGS, the strong acidic environment induced changes in the surface of NAMPs, thereby reducing the electrostatic attraction of NAMPs for metal ions, which promoted the release of heavy metal ions. The dissolution of the mineral particles bonded with metals was also account for the release of metals. This study proves that heavy metals attached on NAMPs can release in the digestive environment and salt water, and provides theoretical basis to the management of the ecological risks combined pollution of heavy metals and NAMPs. In this study, artificially broken macroplastics was used to simulate microplastics, the actual microplastics in the environment should be further studied. Each polymer has a different capacity of adsorption for heavy metals. Further studies are needed to distinguish different plastic polymers, illustrate their bonding and release properties for different heavy metals, and figure out the relation of polymer.

Credit author statement

Gaobin Chen: Conceptualization, Formal analysis, Investigation, Writing – original draft, Rreview & Editing. **Qianmin Fu:** Methodology, Formal analysis, Writing – original draft, Rreview & Editing. **Xiaofei Tan:** Methodology, Supervision, Rreview & Editing. **Hailan Yang:** Methodology, Rreview & Editing. **Yang Luo:** Investigation, Rreview & Editing. **Maocai Shen:** Methodology, Rreview & Editing. **Yanling Gu:** Supervision, Rreview.

Declaration of competing interest

The authors declare that they have no known competing financial interests or personal relationships that could have appeared to influence the work reported in this.

Acknowledgments

This research was financially supported by the National Key R&D Program of China (2020YFC1807600), the Natural Science Foundation of Hunan Province, China (Grant No. 2021JJ30123).

Appendix A. Supplementary data

Supplementary data to this article can be found online at https://doi.org/10.1016/j.envpol.2021.118695.

References

Ajith, N., Arumugam, S., Parthasarathy, S., Manupoori, S., Janakiraman, S., 2020. Global distribution of microplastics and its impact on marine environment-a review. Environ. Sci. Pollut. Res. Int. 27, 25970–25986. https://doi.org/10.1007/s11356-020-09015-5.

Almeida, C.M.R., Manjate, E., Ramos, S., 2020. Adsorption of Cd and Cu to different types of microplastics in estuarine salt marsh medium. Mar. Pollut. Bull. 151, 110797. https://doi.org/10.1016/j.marpolbul.2019.110797.

Barboza, L.G.A., Vieira, L.R., Branco, V., Figueiredo, N., Carvalho, F., Carvalho, C., Guilhermino, L., 2018. Microplastics cause neurotoxicity, oxidative damage and energy-related changes and interact with the bioaccumulation of mercury in the European seabass, Dicentrarchus labrax (Linnaeus, 1758). Aquat. Toxicol. 195, 49–57. https://doi.org/10.1016/j.aquatox.2017.12.008.

Bassegio, C., Campagnolo, M.A., Schwantes, D., Goncalves Junior, A.C., Manfrin, J., Schiller, A.d.P., Bassegio, D., 2020. Growth and accumulation of Pb by roots and shoots of Brassica juncea L. Int. J. Phytoremediation 22, 134–139. https://doi.org/10.1080/15226514.2019.1647406.

Bessaies, H., Iftekhar, S., Doshi, B., Kheriji, J., Ncibi, M.C., Srivastava, V., Sillanpaa, M., Hamrouni, B., 2020. Synthesis of novel adsorbent by intercalation of biopolymer in LDH for the removal of arsenic from synthetic and natural water. J. Environ. Sci. (China) 91, 246–261. https://doi.org/10.1016/j.jes.2020.01.028.

Besson, M., Jacob, H., Oberhaensli, F., Taylor, A., Swarzenski, P.W., Metian, M., 2020. Preferential adsorption of Cd, Cs and Zn onto virgin polyethylene microplastic versus sediment particles. Mar. Pollut. Bull. 156, 111223. https://doi.org/10.1016/j.marpolbul.2020.111223.

Biamis, C., Driscoll, K.O., Hardiman, G., 2021. Microplastic toxicity: a review of the role of marine sentinel species in assessing the environmental and public health impacts. Case Stud. Chem. Environ. Eng. 3 https://doi.org/10.1016/j.cscee.2020.100073.

Brennecke, D., Duarte, B., Paiva, F., Caçador, I., Canning-Clode, J., 2016. Microplastics as vector for heavy metal contamination from the marine environment. Estuar. Coast Shelf Sci. 178, 189–195. https://doi.org/10.1016/j.ecss.2015.12.003.

Browne, M.A., Niven, S.J., Galloway, T.S., Rowland, S.J., Thompson, R.C., 2013. Microplastic moves pollutants and additives to worms, reducing functions linked to health and biodiversity. Curr. Biol. 23, 2388–2392. https://doi.org/10.1016/j.cub.2013.10.012.

Cui, K., He, Y., Jin, S., 2016. Enhanced UV–visible response of bismuth subcarbonate nanowires for degradation of xanthate and photocatalytic reaction mechanism. Chemosphere 149, 245–253. https://doi.org/10.1016/j.chemosphere.2016.01.111.

da Costa Araujo, A.P., de Melo, N.F.S., de Oliveira Junior, A.G., Rodrigues, F.P., Fernandes, T., de Andrade Vieira, J.E., Rocha, T.L., Malafaia, G., 2020. How much are microplastics harmful to the health of amphibians? A study with pristine polyethylene microplastics and Physalaemus cuvieri. J. Hazard Mater. 382, 121066. https://doi.org/10.1016/j.jhazmat.2019.121066.

Desforges, J.-P.W., Galbraith, M., Ross, P.S., 2015. Ingestion of microplastics by zooplankton in the northeast pacific ocean. Arch. Environ. Contam. Toxicol. 69, 320–330. https://doi.org/10.1007/s00244-015-0172-5.

Dong, Y., Gao, M., Song, Z., Qiu, W., 2019. Adsorption mechanism of As(III) on polytetrafluoroethylene particles of different size. Environ. Pollut. 254, 112950. https://doi.org/10.1016/j.envpol.2019.07.118.

El Hadri, H., Gigault, J., Mounicou, S., Grassl, B., Reynaud, S., 2020. Trace element distribution in marine microplastics using laser ablation-ICP-MS. Mar. Pollut. Bull. 160, 111716. https://doi.org/10.1016/j.marpolbul.2020.111716.

Ferreira, P., Fonte, E., Soares, M.E., Carvalho, F., Guilhermino, L., 2016. Effects of multi-stressors on juveniles of the marine fish Pomatoschistus microps: gold nanoparticles, microplastics and temperature. Aquat. Toxicol. 170, 89–103. https://doi.org/10.1016/j.aquatox.2015.11.011.

Fu, Q., Tan, X., Ye, S., Ma, L., Gu, Y., Zhang, P., Chen, Q., Yang, Y., Tang, Y., 2021. Mechanism analysis of heavy metal lead captured by natural-aged microplastics. Chemosphere 270, 128624. https://doi.org/10.1016/j.chemosphere.2020.128624.

Gao, F., Li, J., Sun, C., Zhang, L., Jiang, F., Cao, W., Zheng, L., 2019. Study on the capability and characteristics of heavy metals enriched on microplastics in marine environment. Mar. Pollut. Bull. 144, 61–67. https://doi.org/10.1016/j.marpolbul.2019.04.039.

Guo, X., Wang, J., 2021. Projecting the sorption capacity of heavy metal ions onto microplastics in global aquatic environments using artificial neural networks. J. Hazard Mater. 402, 123709. https://doi.org/10.1016/j.jhazmat.2020.123709.

Guo, Y., Zhu, Z., Qiu, Y., Zhao, J., 2013. Synthesis of mesoporous Cu/Mg/Fe layered double hydroxide and its adsorption performance for arsenate in aqueous solutions. J. Environ. Sci. 25, 944–953. https://doi.org/10.1016/S1001-0742(12)60106-5.

Gupta, P.K., 2016. Fundamentals of Toxicology: Essential Concepts and Applications. Academic Press.

Hao, L., Hu, Y., Zhang, Y., Ping, X., Liu, T., Zhao, Q., Lu, Y., Liu, J., 2021. Flexible TiO2 nanograss array film decorated with BiOI nanoflakes and its greatly boosted photocatalytic activity. Ceram. Int. 47, 7845–7852. https://doi.org/10.1016/j.ceramint.2020.11.131.

Hayati-Ashtiani, M., 2011. Characterization of nano-porous bentonite (montmorillonite) particles using FTIR and BET-BJH analyses. Part. Part. Syst. Char. 28, 71–76.

Hodson, M.E., Duffus-Hodson, C.A., Clark, A., Prendergast-Miller, M.T., Thorpe, K.L., 2017. Plastic bag derived-microplastics as a vector for metal exposure in terrestrial invertebrates. Environ. Sci. Technol. 51, 4714–4721. https://doi.org/10.1021/acs.est.7b00635.

Jiang, L., Zhang, L., Cui, C., Zhang, J., Liu, G., Song, J., 2019. Efficient degradation of phenol using Sn4+ doped FeOCl as photo-Fenton catalyst. Mater. Lett. 240, 30–34. https://doi.org/10.1016/j.matlet.2018.12.112.

Kalcikova, G., Skalar, T., Marolt, G., Jemec Kokalj, A., 2020. An environmental concentration of aged microplastics with adsorbed silver significantly affects aquatic organisms. Water Res. 175, 115644. https://doi.org/10.1016/j.watres.2020.115644.

Li, C., Yao, Y., 2020. Synthesis of bimetallic core-shell silver-copper nanoparticles decorated on reduced graphene oxide with enhanced electrocatalytic performance. Chem. Phys. Lett. 761 https://doi.org/10.1016/j.cplett.2020.137726.

Liu, J., Zhang, T., Tian, L., Liu, X., Qi, Z., Ma, Y., Ji, R., Chen, W., 2019. Aging significantly affects mobility and contaminant-mobilizing ability of nanoplastics in saturated loamy sand. Environ. Sci. Technol. 53, 5805–5815. https://doi.org/10.1021/acs.est.9b00787.

Liu, P., Lu, K., Li, J., Wu, X., Qian, L., Wang, M., Gao, S., 2020. Effect of aging on adsorption behavior of polystyrene microplastics for pharmaceuticals: adsorption mechanism and role of aging intermediates. J. Hazard Mater. 384, 121193. https://doi.org/10.1016/j.jhazmat.2019.121193.

Long, M., Moriceau, B., Gallinari, M., Lambert, C., Huvet, A., Raffray, J., Soudant, P., 2015. Interactions between microplastics and phytoplankton aggregates: impact on their respective fates. Mar. Chem. 175, 39–46. https://doi.org/10.1016/j.marchem.2015.04.003.

Ma, Y.D., Gao, J.F., Chen, X.W., Kong, L.B., 2021. Regulation of the mesopore proportion of porous carbon for optimizing the performance of electric double layer capacitors. J. Energy Storage 35. https://doi.org/10.1016/j.est.2021.102299.

Ma, Y., Zhou, Y., Sun, Y., Chen, H., Xiong, Z., Li, X., Shen, L., Liu, Y., 2019. Tunable magnetic properties of Fe3O4/rGO/PANI nanocomposites for enhancing microwave absorption performance. J. Alloys Compd. 796, 120–130. https://doi.org/10.1016/j.jallcom.2019.04.310.

Misran, H., Salim, M.A., Ramesh, S., 2018. Effect of Ag nanoparticles seeding on the properties of silica spheres. Ceram. Int. 44, 5901–5908. https://doi.org/10.1016/j.ceramint.2017.12.118.

Mukasa-Tebandeke, I., Wasajja-Navoyojo, S.A., Ntale, M., 2016. Analysis, characterization and bleaching properties of smectite from iliri road swelling clays in north eastern Uganda, leached in different acids. Bull. Pure Appl. Sci. Geol. 35, 39–78.

Nikitin, T., Khriachtchev, L., 2015. Optical and structural properties of Si nanocrystals in SiO2 films. Nanomaterials 5, 614–655. https://doi.org/10.3390/nano5020614.

Qiao, M., Ran, Q., Wu, S., 2018. Novel star-like surfactant as dispersant for multi-walled carbon nanotubes in aqueous suspensions at high concentration. Appl. Surf. Sci. 433, 975–982. https://doi.org/10.1016/j.apsusc.2017.10.138.

Rozman, U., Turk, T., Skalar, T., Zupancic, M., Celan Korosin, N., Marinsek, M., Olivero-Verbel, J., Kalcikova, G., 2021. An extensive characterization of various environmentally relevant microplastics - material properties, leaching and ecotoxicity testing. Sci. Total Environ. 773, 145576. https://doi.org/10.1016/j.scitotenv.2021.145576.

Sahu, S., Behera, B., Maiti, T.K., Mohapatra, S., 2012. Simple one-step synthesis of highly luminescent carbon dots from orange juice: application as excellent bio-imaging agents. Chem. Commun. (Camb) 48, 8835–8837. https://doi.org/10.1039/c2cc33796g.

Salehi, M., Jafvert, C.T., Howarter, J.A., Whelton, A.J., 2018. Investigation of the factors that influence lead accumulation onto polyethylene: implication for potable water plumbing pipes. J. Hazard Mater. 347, 242–251. https://doi.org/10.1016/j.jhazmat.2017.12.066.

Sethumadhavan, V., Zuber, K., Bassell, C., Teasdale, P.R., Evans, D., 2020. Hydrolysis of doped conducting polymers. Commun. Chem. 3 https://doi.org/10.1038/s42004-020-00404-y.

Sharma, S., Nagpal, A.K., Kaur, I., 2019. Appraisal of heavy metal contents in groundwater and associated health hazards posed to human population of Ropar wetland, Punjab, India and its environs. Chemosphere 227, 179–190. https://doi.org/10.1016/j.chemosphere.2019.04.009.

Shen, M., Zhu, Y., Zhang, Y., Zeng, G., Wen, X., Yi, H., Ye, S., Ren, X., Song, B., 2019. Micro(nano)plastics: unignorable vectors for organisms. Mar. Pollut. Bull. 139, 328–331. https://doi.org/10.1016/j.marpolbul.2019.01.004.

Sun, Y., Wen, D., 2020. Physically transient random number generators based on flexible carbon nanotube composite threshold switching. J. Alloys Compd. 844 https://doi.org/10.1016/j.jallcom.2020.156144.

Tang, S., Lin, L., Wang, X., Feng, A., Yu, A., 2020. Pb(II) uptake onto nylon microplastics: interaction mechanism and adsorption performance. J. Hazard Mater. 386, 121960. https://doi.org/10.1016/j.jhazmat.2019.121960.

Vroom, R.J.E., Koelmans, A.A., Besseling, E., Halsband, C., 2017. Aging of microplastics promotes their ingestion by marine zooplankton. Environ. Pollut. 231, 987–996. https://doi.org/10.1016/j.envpol.2017.08.088.

Wang, F., Yang, W., Cheng, P., Zhang, S., Zhang, S., Jiao, W., Sun, Y., 2019. Adsorption characteristics of cadmium onto microplastics from aqueous solutions. Chemosphere 235, 1073–1080. https://doi.org/10.1016/j.chemosphere.2019.06.196.

Wright, S.L., Rowe, D., Thompson, R.C., Galloway, T.S., 2013. Microplastic ingestion decreases energy reserves in marine worms. Curr. Biol. 23, R1031–R1033. https://doi.org/10.1016/j.cub.2013.10.068.

Wu, B., Wu, X., Liu, S., Wang, Z., Chen, L., 2019. Size-dependent effects of polystyrene microplastics on cytotoxicity and efflux pump inhibition in human Caco-2cells. Chemosphere 221, 333–341. https://doi.org/10.1016/j.chemosphere.2019.01.056.

Ye, S., Cheng, M., Zeng, G., Tan, X., Wu, H., Liang, J., Shen, M., Song, B., Liu, J., Yang, H., Zhang, Y., 2020. Insights into catalytic removal and separation of attached metals from natural-aged microplastics by magnetic biochar activating oxidation process. Water Res. 179, 115876. https://doi.org/10.1016/j.watres.2020.115876.

Yin, L., Chen, B., Xia, B., Shi, X., Qu, K., 2018. Polystyrene microplastics alter the behavior, energy reserve and nutritional composition of marine jacopever (Sebastes schlegelii). J. Hazard Mater. 360, 97–105. https://doi.org/10.1016/j.jhazmat.2018.07.110.

Yin, Z., Liu, Y., Tan, X., Jiang, L., Zeng, G., Liu, S., Tian, S., Liu, S., Liu, N., Li, M., 2019. Adsorption of 17β-estradiol by a novel attapulgite/biochar nanocomposite : characteristics and influencing factors. Process Saf. Environ. Protect. 121, 155–164. https://doi.org/10.1016/j.psep.2018.10.022.

Young, T.F., Chen, C.P., Liou, J.F., Yang, Y.L., Chang, T.C., 2000. Study on the Si–Si vibrational states of the near surface region of porous silicon. J. Porous Mater. 7, 339–343. https://doi.org/10.1023/A:1009622601723.

Zemberyova, M., Bartekova, J., Hagarova, I., 2006. The utilization of modified BCR three-step sequential extraction procedure for the fractionation of Cd, Cr, Cu, Ni, Pb and Zn in soil reference materials of different origins. Talanta 70, 973–978. https://doi.org/10.1016/j.talanta.2006.05.057.

Zhang, J., Yang, M., Lian, Y., Zhong, M., Sha, J., Liu, G., Zhao, X., Liu, S., 2019. Ce3+ self-doped CeOx/FeOCl: an efficient Fenton catalyst for phenol degradation under mild conditions. Dalton Trans. 48, 3476–3485. https://doi.org/10.1039/C8DT04269A.

Zhao, S., Ding, H., Chen, J., Yang, C., Xian, X., 2021. Facile synthesis of CNTs@TiO2 composites by solvothermal reaction for high-rate and long-life lithium-ion batteries. J. Phys. Chem. Solid. 152 https://doi.org/10.1016/j.jpcs.2021.109950.

Zhou, Y., Liu, X., Wang, J., 2019. Characterization of microplastics and the association of heavy metals with microplastics in suburban soil of central China. Sci. Total Environ. 694, 133798. https://doi.org/10.1016/j.scitotenv.2019.133798.

Zhou, Y.F., Yang, Y.Y., Liu, G.H., He, G., Liu, W.Z., 2020. Adsorption mechanism of cadmium on microplastics and their desorption behavior in sediment and gut environments: the roles of water pH, lead ions, natural organic matter and phenanthrene. Water Res. 184 https://doi.org/10.1016/j.watres.2020.116209.